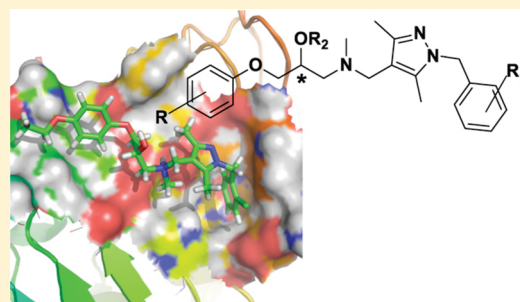


Development of β -Amino Alcohol Derivatives That Inhibit Toll-like Receptor 4 Mediated Inflammatory Response as Potential AntisepticsSherry A. Chavez,^{†,||} Alexander J. Martinko,^{†,||} Corinna Lau,[‡] Michael N. Pham,[†] Kui Cheng,[†] Douglas E. Bevan,[†] Tom E. Mollnes,^{‡,§} and Hang Yin^{*,†}[†]Department of Chemistry and Biochemistry, University of Colorado at Boulder, Boulder, Colorado 80309, United States[‡]Research Laboratory, Nordland Hospital, Bodø NO-8092, Norway[§]University of Tromsø, Tromsø, NO-9037, Norway

S Supporting Information

ABSTRACT: Toll-like receptor 4 (TLR4) induced proinflammatory signaling has been directly implicated in severe sepsis and represents an attractive therapeutic target. Herein, we report our investigations into the structure–activity relationship and preliminary drug metabolism/pharmacokinetics study of β -amino alcohol derivatives that inhibit the TLR4 signaling pathway. Lead compounds were identified from in vitro cellular examination with micromolar potency for their inhibitory effects on TLR4 signaling and subsequently assessed for their ability to suppress the TLR4-induced inflammatory response in an ex vivo whole blood model. In addition, the toxicology, specificity, solubility, brain–blood barrier permeability, and drug metabolism of several compounds were evaluated. Although further optimizations are needed, our findings lay the groundwork for the future drug development of this class of small molecule agents for the treatment of severe sepsis.



INTRODUCTION

The protective functions of innate immunity rely principally on the ability of an organism to discriminate between endogenous signals and exogenous danger signals of microbial origin.^{1,2} Toll-like receptors (TLRs) are a conserved family of integral membrane proteins, which maintain this essential role of innate immunity. At least 10 TLRs have been identified in human and 13 in mice, each of which recognizes its own group of conserved pathogen associated molecular patterns (PAMPs).

Toll-like receptor 4 (TLR4), the first of the TLR family to be identified, along with its accessory protein myeloid differentiation factor 2 (MD2), forms a heterodimeric complex. This complex specifically recognizes lipopolysaccharide (LPS), a structurally variant component of Gram-negative bacterial cell walls.^{3,4} Once LPS is recognized, a homoheterodimer consisting of two TLR4–MD2–LPS complexes is formed. This homoheterodimer confers an intracellular signaling cascade that results in downstream activation and nuclear translocation of the transcription factor, nuclear factor κ B (NF- κ B).⁵ Nuclear translocation of NF- κ B results in subsequent transcriptional up-regulation of proinflammatory cytokines such as interleukin 1 (IL-1), interleukin 6 (IL-6), and tumor necrosis factor- α (TNF- α).^{2,5} Given the key role TLR4 plays in regulating cytokines, inhibition of TLR4-mediated signaling is an appealing target for therapeutic development.

Although TLR4-induced cytokine signaling is generally advantageous in fighting infection, TLR4 signaling dysregulation

has been directly implicated in a myriad of diseases including sepsis and neuropathic pain.^{6–9} Severe sepsis poses a particular threat as a serious medical condition characterized by a systemic inflammation state that results in over 200 000 attributed deaths annually in the United States.¹⁰ Several groups have attempted to design potent antiseptics agents by employing the strategy of developing LPS-mimicking antagonists of TLR4.^{11,12} One advantage of deriving inhibitors by this method is that antagonists can be developed by rationally modifying the active glycolipid component of LPS to optimize drug efficacy. The disadvantage posed is that these LPS mimetics are typically too large to render the desired pharmacological properties.¹³ A recent example of such a design is eritoran, a lipid-A mimetic with high affinity for TLR4. Although it reached phase III clinical trials as an antiseptics agent, eritoran failed to demonstrate sufficient efficacy in late stage human trials. An alternative strategy, which has the potential for high specificity and bioavailability, is to design low-molecular-weight inhibitors.^{14,15} By use of this strategy, several small molecules have been developed to target and antagonize TLR4. To the best of our knowledge, none have successfully advanced through late stage clinical trials.^{16–18} TAK-242 (resatorvid), the most successful TLR4-binding small molecule antagonist, reached phase III clinical trials as an antiseptics agent, but studies were recently discontinued because of a failure to suppress cytokine

Received: March 23, 2011

Published: May 17, 2011

levels in patients despite showing promising preclinical efficacy in animal models.^{19–21} These results might suggest that the current approaches to targeting the TLR4 receptor are flawed. There is an urgent need to develop and validate novel strategies to target the TLR4 pathway for antiseptic therapeutic development.

Using an *in silico* screen, we have identified β -amino alcohol derivatives (1) as generic inhibitors that disrupt the TLR4/MD2 complex formation.^{22,23} These inhibitors were shown to be effective at suppressing NF- κ B activation in TLR4-overexpressing human embryonic kidney (HEK) 293.²² Herein, we further these studies on the preparation, optimization, and biological evaluation of β -amino alcohol derivatives that inhibit LPS-induced inflammation in whole blood. Our findings may lay the groundwork for a new drug development strategy for the treatment of severe sepsis by targeting the TLR4/MD2 interface and suggest a class of prototype small molecule agents.

INHIBITOR PREPARATION

Synthesis of β -Amino Alcohol Derivatives. A β -amino alcohol of type 1 can be derived from a substituted aryloxy epoxide of type 2 and a functionalized pyrazole compound such as 3 (Figure 1). The epoxide fragments 2 were derived from epichlorohydrin and a phenol derivative, 4. To generate an amine

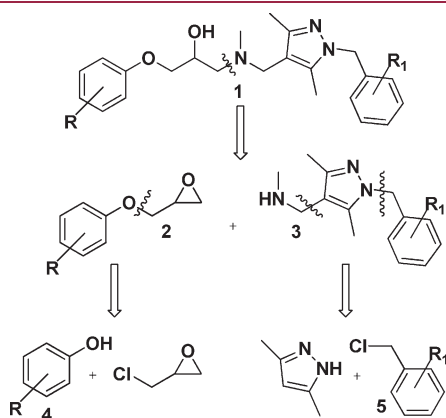
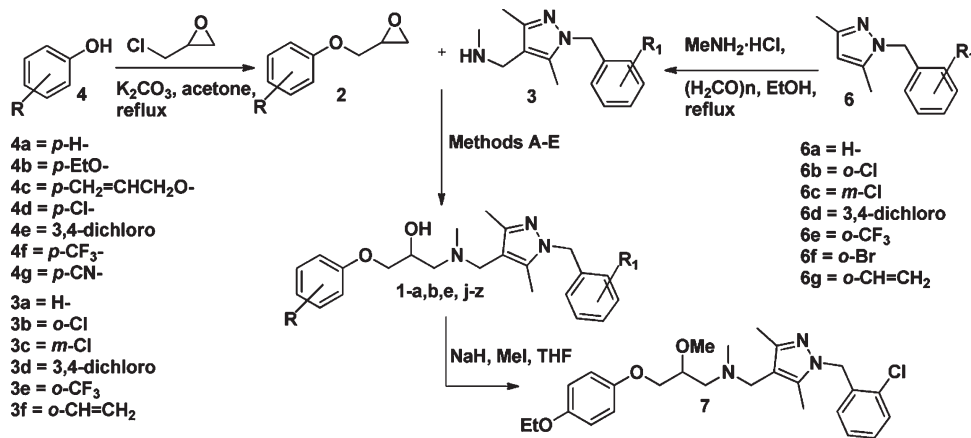


Figure 1. Retrosynthesis of pyrazole containing β -amino alcohols.

Scheme 1. Synthesis of β -Amino Alcohol Derivatives^a



^a Method A = EtOH, reflux. Method B = MeCN, K₂CO₃, reflux. Method C = toluene, reflux. Method D = EtOH, microwave 200 W, 140 °C. Method E = MeCN, K₂CO₃, microwave 200 W, 140 °C. See Experimental Section for specific methods and yields.

fragment of type 3, a Mannich-type reaction was utilized to further functionalize a 3,5-dimethyl-1*H*-pyrazole intermediate where paraformaldehyde provided the methylene source and methylamine hydrochloride.²²

The desired aryloxyoxiranes (2) were synthesized via the reaction of the sodium salt of substituted phenols (4) with epichlorohydrin (Scheme 1).²⁴ Selective incorporation of an allyl ether group was accomplished starting from hydroquinone (R = OH, K₂CO₃, allyl bromide, acetone) to yield the epoxide 2c after addition to epichlorohydrin.²⁵

The functionalized heterocycles of type (3) were synthesized using previously established methodology.²¹ Preparation of analogues containing a styrene functionality was achieved using (2-bromobenzyl)pyrazole (6f). A palladium-catalyzed Stille coupling, using Pd(PPh₃)₄ and tributylvinyltin in toluene, generated the styrenepyrazole intermediate (6g).²⁶ A Mannich coupling with methylamine and paraformaldehyde formed the amine derivative 3f.

Preparation of the β -aminohydroxyl compounds was carried out by condensing amino substituted pyrazoles with the aryloxyoxiranes. We found that by subjecting 1 equiv of an aryloxyoxirane (2) and a slight excess (1.1 equiv) of the functionalized secondary amine (3) to different reaction conditions, we could improve the isolated yields of the β -aminohydroxyl compounds. Because of the limited solubility of many of the starting materials, ethanol was commonly used as the solvent. Unfortunately, we frequently observed the addition of ethanol to the oxirane under refluxing conditions. We successfully suppressed this competing reaction in several reactions with the use of either acetonitrile²⁷ or toluene.²⁸

Flitsch and co-workers reported good yields of amino alcohols via the ring-opening of epoxides with a variety of amines under microwave irradiation conditions.²⁹ Conducting the coupling reaction under similar conditions (140 °C, 200 W) using a variety of solvent systems resulted in a significant decrease in reaction times (24–48 h to less than 1 h) and generated excellent yields. We found that either acetonitrile or EtOH worked equally well under the microwave irradiation conditions with only minor traces of the EtOH addition products.

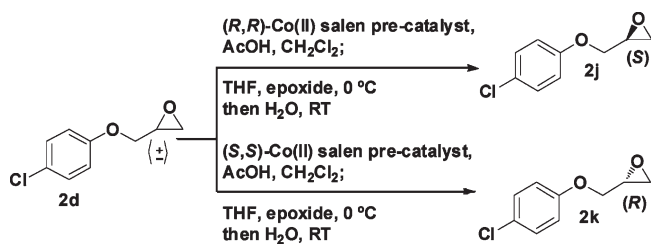
In order to explore the role the alcohol group of 1 plays in binding to TLR4, compound 1j was methylated utilizing the standard conditions (MeI, NaH) to generate the methyl ether 7.

Synthesis of Chiral Derivatives. In order to determine if the stereochemistry of the hydroxyl group was essential to the ligand/receptor interaction, the enantiomers of **1s** ($R = p\text{-Cl}$, $R_1 = o\text{-Cl}$) were synthesized (Scheme 2). Previously synthesized enantiomers of **1j** ($R = p\text{-OEt}$, $R_1 = o\text{-Cl}$) were also prepared for direct comparison in the current biological assays. Published reports utilized Jacobsen's hydrokinetic resolution methodology to generate enantioenriched epoxides that could then be opened with the secondary amine nucleophile.³⁰ The active (R,R)-(salen)Co(III)OAc catalyst was generated in situ by the aerobic oxidation of [(R,R)- N,N' -bis(3,5-di-*tert*-butylsalicylidene)-1,2-cyclohexanediamino]cobalt(II) in the presence of acetic acid. Treatment of the desired racemic epoxides (**2b** and **2d**) with (R,R)-(salen)Co(III)OAc catalyst and water yielded the (S)-enantioenriched epoxides (**2h**, $R = p\text{-OEt}$ and **2j**, $R = p\text{-Cl}$) and the ring opened (R)-diol products. The corresponding (S,S)-(salen)Co(III)OAc catalyst was utilized to generate the desired (R)-epoxides (**2i**, $R = p\text{-OEt}$ and **2k**, $R = p\text{-Cl}$).^{31,32} We later found that quenching the reaction with pyridinium *p*-toluenesulfonate (PPTS) (4 equiv of PPTS/mmol of catalyst) in a 1:1 mixture of MeCN and CH_2Cl_2 removed the catalyst prior to purification and increased the chiral epoxide yields.^{33,34}

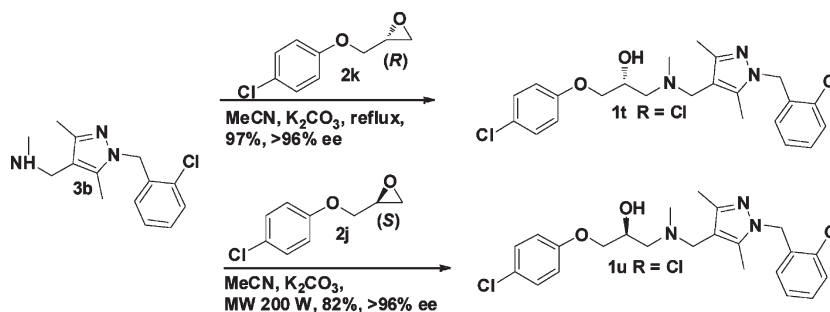
Generation of the chiral β -amino alcohols (**1l**, **1k**, **1u**, and **1t**) was accomplished by using similar reaction conditions to their racemic counterparts. We found that both toluene and acetonitrile were effective solvents for these coupling. The addition of a heterogeneous base K_2CO_3 increased the overall yields, and the use of microwave conditions did not affect the enantioselectivity or the yields (Scheme 3). The enantiomeric excess was determined to be greater than 96% by chiral HPLC analysis for each of the derivatives regardless of the reaction conditions.

Synthesis of Cyclic Derivatives. A commonly used strategy to improve the potency of flexible small molecule inhibitors is to prepare the cyclic derivatives with increased rigidity, which reduces the entropic penalty upon binding to their protein receptor.³⁵ The macrocycle scaffold (**8**) was designed based on

Scheme 2. Synthesis of Chiral Epoxides



Scheme 3. Synthesis of Enantioenriched β -Amino Alcohol



one of our more active linear compounds, **1q**, and is properly substituted to undergo ring closing metathesis through a convenient annulation method (Scheme 4). The desired macrocyclic compound **8** was synthesized by cyclizing the linear precursor **1q** using Grubbs II catalyst with a 52% yield and greater than 1:10 *E/Z* selectivity after purification.³⁶

■ BIOLOGICAL EVALUATION

Inhibition of the LPS-Induced TLR4 Activation in Macrophage Cells. The potency of the β -amino alcohol derivatives as inhibitors of TLR4 signaling was determined by monitoring the reduction of LPS-induced production of nitric oxide (NO) in RAW 264.7 macrophage cells. The IC_{50} values and the margin of error were determined by a modified Kou-type method from experiments conducted in quadruplicate.³⁷

The compound that lacked substitution on either of the aryl rings (e.g., **1a**, $R = R_1 = \text{H}$) was ineffective at suppressing NO signaling (Table 1). For this reason, compound **1a** was utilized as a negative control for this assay. Mild suppression of NO production was observed when substitutions were made to either of the benzyl rings (**1e** $\text{IC}_{50} = 51.8 \pm 5.8 \mu\text{M}$ and **1b** $\text{IC}_{50} = 64.3 \pm 0.1 \mu\text{M}$), suggesting that substitution of both aryl rings is needed for activity.

The small structural variations between compounds **1b**, **1c**, **1e**, and **1j** and the corresponding biological activity gave preliminary indications that a combination of electronic properties and lipophilicity may play a role in improving the biological activity. Several additional compounds were synthesized to further explore the effect of substitution located on the aromatic ring derived from the epoxide fragment.

By use of **1j** as the prototype compound ($R = p\text{-OEt}$, $R_1 = o\text{-Cl}$; $\text{IC}_{50} = 27.8 \pm 0.3 \mu\text{M}$), several analogues were prepared in which the *R* group was modified to explore the influence of electronics and lipophilicity. Synthesis of derivative **1v**, which incorporated an additional chloride substitution ($R = 3,4\text{-dichloro-}$, $R_1 = o\text{-Cl}$), resulted in a slight decrease of activity from compound **1s** ($R = p\text{-Cl}$, $R_1 = o\text{-Cl}$; $\text{IC}_{50} = 16.1 \pm 1.1 \mu\text{M}$). Increasing the lipophilicity ($R = p\text{-CF}_3$, $R_1 = o\text{-Cl}$, **1y**) generated a slight loss of NO suppression compared with that of **1s**. Interestingly, significant loss of activity was observed with compound **1z** where $R = p\text{-CN}$ ($\text{IC}_{50} = 52.7 \pm 2.6 \mu\text{M}$).

On the basis of the current SAR set, it would appear that an electron withdrawing group versus an electron donating group on the phenoxy ring at the para position favors activity (e.g., **1s** [$R = p\text{-Cl}$] > **1j** [$R = p\text{-OEt}$] > **1a** [$R = \text{H}$]). Although there seems to be a slight dependence on the electronic nature of the aromatic ring, activity appears to be influenced more by increased lipophilicity.

Scheme 4. Synthesis of a Cyclic Derivative

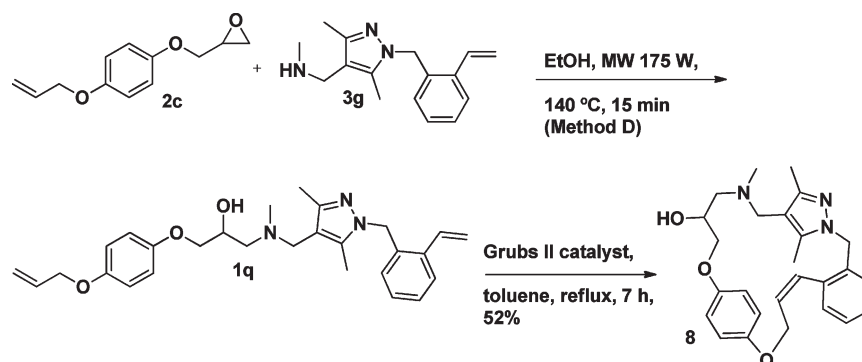


Table 1. Suppression of the LPS-Induced NO Production in RAW 264 Macrophage Cells

	*	R	R ₁	R ₂	IC ₅₀ (μM)
1a	±	H	H	H	>100
1b	±	H	<i>o</i> -Cl	H	64.3 ± 0.1
1c	±	<i>p</i> -CH ₃ OCH ₂ CH ₂ -	<i>o</i> -Cl	H	57.3 ± 2.8
1d	±	<i>o</i> -CH ₃ O-	<i>o</i> -Cl	H	92.5 ± 0.8
1e	±	<i>p</i> -CH ₃ CH ₂ O-	H	H	51.8 ± 5.8
1f	±	<i>p</i> -CH ₃ CH ₂ O-	<i>o</i> -CH ₃	H	47.7 ± 3.7
1g	±	<i>p</i> -CH ₃ CH ₂ O-	<i>o</i> -OCH ₃	H	>100
1h	±	<i>p</i> -CH ₃ CH ₂ O-	<i>p</i> -OCH ₃	H	67.6 ± 0.3
1i	±	<i>p</i> -CH ₃ CH ₂ O-	<i>o</i> -F	H	47.7 ± 2.7
1j	±	<i>p</i> -CH ₃ CH ₂ O-	<i>o</i> -Cl	H	27.8 ± 0.3
1k	(R)	<i>p</i> -CH ₃ CH ₂ O-	<i>o</i> -Cl	H	24.8 ± 3.0
1l	(S)	<i>p</i> -CH ₃ CH ₂ O-	<i>o</i> -Cl	H	24.3 ± 3.7
7	±	<i>p</i> -CH ₃ CH ₂ O-	<i>o</i> -Cl	CH ₃	19.8 ± 0.1
1m	±	<i>p</i> -CH ₃ CH ₂ O-	<i>m</i> -Cl	H	16.5 ± 0.8
1n	±	<i>p</i> -CH ₃ CH ₂ O-	3,4-dichloro	H	21.8 ± 3.1
1o	±	<i>p</i> -CH ₃ CH ₂ O-	<i>o</i> -CH=CH ₂	H	24.7 ± 9.0
1p	±	<i>p</i> -CH ₃ CH ₂ O-	<i>o</i> -CF ₃	H	32.1 ± 2.2
1q	±	<i>p</i> -CH ₂ =CHCH ₂ O-	<i>o</i> -CH=CH ₂	H	23.1 ± 1.1
1r	±	<i>p</i> -CH ₂ =CHCH ₂ O-	<i>o</i> -Cl	H	44.6 ± 7.0
1s	±	<i>p</i> -Cl-	<i>o</i> -Cl	H	16.1 ± 1.1
1t	(R)	<i>p</i> -Cl-	<i>o</i> -Cl	H	15.5 ± 0.9
1u	(S)	<i>p</i> -Cl-	<i>o</i> -Cl	H	15.6 ± 0.6
1v	±	3,4-dichloro	<i>o</i> -Cl	H	20.1 ± 0.1
1w	±	<i>p</i> -Cl-	<i>o</i> -CH=CH ₂	H	23.2 ± 0.7
1x	±	<i>p</i> -CF ₃ -	<i>o</i> -CF ₃	H	27.3 ± 0.0
1y	±	<i>p</i> -CF ₃ -	<i>o</i> -Cl	H	23.7 ± 2.6
1z	±	<i>p</i> -CN-	<i>o</i> -Cl	H	52.7 ± 2.6

The effect of substitution on the aromatic ring attached to the pyrazole ring was also studied. Starting again from **1j** as a baseline, the R group was maintained as the *p*-OEt functionality and the R₁ substituent was varied. The use of a methyl group at the ortho position (**1f**) resulted in a compound with activity similar to that of the monosubstituted compound **1e** (R = *p*-OEt,

R₁ = H). Addition of an *o*-OMe group (**1g**) gave a compound with no detectable NO suppression. Although relocating the methoxy group to the para position (**1h**) regenerated some activity (IC₅₀ = 67.6 ± 0.3 μM) the increase in potency was not significant enough to justify further exploration of electron donating groups on the amine fragment.

Modification of *o*-R₁ to a fluorine substituent (**1i**) also did not improve activity. However, incorporation of a more lipophilic, electron withdrawing group such as chlorine (**1j**) reduced the IC₅₀ to nearly half of that seen with fluorine (47.7 ± 2.7 μM compared to 27.8 ± 0.3 μM). Relocating the chlorine substituent to the meta position (**1m**) further improved the IC₅₀ to 16.5 ± 0.8 μM, which is comparable to the IC₅₀ of compound **1s**. Introducing disubstitution, e.g., R₁ = 3,4-dichloro (**1v**), however, did not significantly affect the NO suppression compared to the monochloro derivative.

As seen with the modifications made to phenol group, the addition of an *o*-CF₃ group resulted in a modest decrease in activity (**1p**, IC₅₀ = 31.1 ± 2.2 μM) compared to that of **1j**. Interestingly, when a vinyl group (**1o**) was incorporated into the structure, the inhibitory potency was reduced to an IC₅₀ of 24.7 ± 9.0 μM. These results imply that the ortho position may be more sensitive to sterics than to electronics.

The effect of the hydroxyl group's stereochemistry on NO production was also investigated. Surprisingly, no significant difference in activity between the racemic derivatives and their stereoisomers (**1j**, **1k**, and **1l**) and (**1s**, **1t**, and **1u**) was observed. The results suggest that the role of the alcohol in the small molecule–protein interaction remains unclear and may not be critical for potency. This hypothesis was supported by the methyl ether analogue **7**. The ether derivative demonstrated reasonable activity with an IC₅₀ of 19.8 ± 0.1 μM, implying that an alcohol substitution may not be essential but the C–O– functionality may be important.

An interesting result was obtained with the macrocyclic compound **8**. Compared to the acyclic system (**1q**, IC₅₀ = 23.1 ± 1.1 μM), the macrocycle retained its potency (IC₅₀ = 16.0 ± 2.0 μM), suggesting the possibility of an alternative scaffold.

Inhibition of Inflammatory Response in Human Whole Blood. The biological properties of compounds **1j** and **1a** were further investigated in an effort to determine if this class of compounds would be suitable for further studies as antiseptics agents.³⁸ In human whole blood, **1j** and the control compound **1a** showed differential efficiency in inhibiting the LPS-induced cytokine release. Compound **1j** was more effective at reducing IL-8 secretion than **1a**, and this difference was significant at

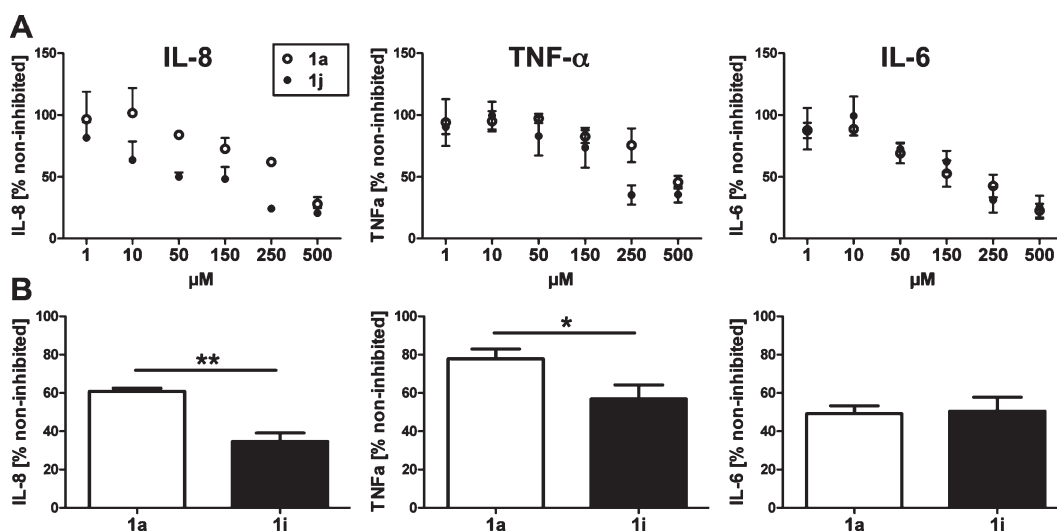


Figure 2. (A) Dose-dependent inhibitory effects of **1a** and **1j** on LPS-mediated cytokine release in human whole blood. (B) Inhibitory effects of compounds **1a** and **1j** at a fixed concentration of 250 μM on LPS-induced cytokine release in human whole blood. Significant difference between the two compounds was observed for inhibiting IL-8 and TNF α but not for IL-6. (** $p < 0.01$, * $p < 0.05$, t test).

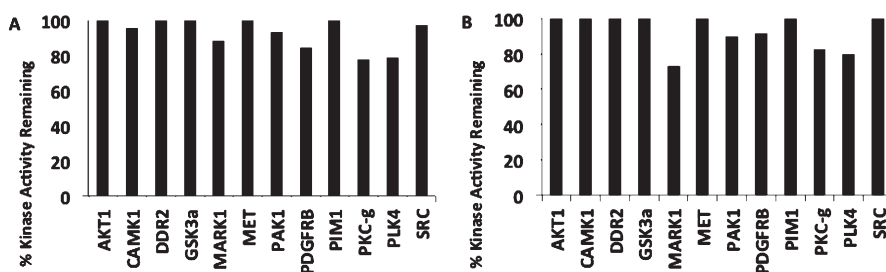


Figure 3. Kinase selectivity screen for **1j** (28 μM) and **1s** (16 μM). Both compounds were profiled against a panel of 12 kinases using the KinaseSeeker assay. (A) Treatment with **1j** resulted in retention of >95% activity for a majority of the kinases, and the most inhibited kinase, PKC- γ , was inhibited by 22.4%. (B) Treatment with **1s** also resulted in the retention of 95% activity for a majority of the kinases, and the most inhibited kinase, MARK1, was inhibited by 26.7%.

concentrations of 50 and 250 μM ($p < 0.05$, t test) (Figure 2A and Figure 2B). Suppression of TNF α release was also observed for **1j** at a dose of 250 μM . However, at 500 μM , both compounds reduced the levels of all of the studied cytokines equally well, suggesting that nonspecific inhibition becomes prevalent at this concentration. These inhibitory affects by **1j** have also been shown to be cytokine-specific. For example, **1j** and **1a** had no observable differences in their inhibitory effects on IL-6 cytokine release.

Compound **1j** reduced the plasma levels of IL-8 to 35% and those of TNF α and IL-6 to 57% and 50%, respectively, at 250 μM . These data are consistent with the estimated IC_{50} values for compound **1j** of 110.5 μM for IL-8, 315.6 μM for TNF- α , and 318.4 μM for IL-6 using the human whole blood model and the secretion of the respective cytokines. The elevated IC_{50} values seen in the whole blood assay compared to the results derived from the cell-culture based assays are perhaps due to the complexity of the ex vivo whole blood system. Consistent with the in vitro assay results, the control compound **1a** showed a significantly lower potency to inhibit the inflammatory response in the whole blood model. Importantly, no agonistic effects with respect to cytokine release or hemolysis in the presence of up to 1 mM of either compound were observed. Taken together, our observations imply that **1j** is effective to suppress LPS-induced inflammatory response in human whole blood.

Drug Metabolism/Pharmacokinetics (DMPK). To preliminarily evaluate the drug potential of **1j**, the metabolic stability, blood–brain barrier (BBB) permeability, and lipophilicity were investigated. To determine the lipophilicity of **1j**, the octanol/water distribution coefficient was measured at the physiologically relevant pH of blood serum (pH 7.4). The $\log D$ of a drug at pH 7.4 is known as a predictor of ADME/TOX properties. The $\log D$ of **1j** was determined to be 3.36, a value marginally above the optimum for drug development but still within a functional range, showing potential for a balance of permeability and solubility.^{39,40}

The BBB permeability of **1j** was evaluated using the MDR1-MDCK permeability assay, a cell culture model system shown to be an accurate predictor of BBB penetration potential. To determine penetration efficiency, the ability of **1j** to pass through an MDR1-MDCK monolayer in both the apical to basolateral and basolateral to apical directions was measured. At 5 μM , **1j** was determined to have a brain–blood barrier permeability classification of “high”.

The metabolic stability of **1j** was also evaluated. The intrinsic clearance (CL_{int}) values of **1j** (1 μM) were determined in the presence of human liver microsomes and human S9 fractions as well as rat S9 fractions. The observed values of CL_{int} in each system were determined to be >0.70, 0.3, and >0.35 (mL/min)/mg

protein, respectively. These data suggest that **1j** is likely to be metabolized in the liver at a relatively rapid rate. Generally, rapid metabolism for a drug candidate is undesirable, and this issue should be addressed as SAR studies continue.

Further, a preliminary cytochrome P450 (CYP) screening was also conducted. Compound **1j** was tested for its ability to inhibit four key cytochrome enzymes involved in drug metabolism. The IC₅₀ values for CYP1A2, CYP2C9, CYP2C19, and CYP2D6 were found to be greater than 100, 43, 20, and 32 μM, respectively. These data, in conjunction with the metabolism results, indicate that further optimization of the specificity of **1j** is needed before advancement to more clinically relevant *in vivo* models can be considered.

Specificity and Toxicity Tests. The β-amino alcohol derivatives were further examined for their specificity to TLR4 and screened against 12 representative kinases (AKT1, CAMK1, DDR2, GSK-3α, MAPK1, MET, PAK1, PDGFRB, PIM1, PKC-γ, PLK4, and SRC). The two active lead compounds, **1j** and **1s**, were screened (Figure 3) using a KinaseSeeker assay (a luciferase fragment complementation assay that provides a direct measurement of their interactions with each respective kinase). Neither **1j** nor **1s** inhibited a kinase by more than 27% at their respective IC₅₀ concentrations determined in the RAW264.7 macrophage cells, while the majority of the kinases examined retained >95% of their activity. The results suggest that the active dose of **1j** or **1s** required for TLR4 inhibition does not substantially perturb the activity of these biologically essential enzymes.

Toxicity assessments for the β-amino alcohol derivatives were carried out using a variety of methods. We have observed that the cell toxicity was variable and cell line dependent (Supporting Information Figures 1 and 2). Most importantly, negligible hemolysis was observed at concentrations as high as 1 mM in human whole blood.

CONCLUSIONS

We have reported initial results regarding the development of a series of low molecular weight β-amino alcohol derivatives that appear to suppress TLR4-mediated inflammation response. Preliminary structure–activity relationship studies revealed that variation of functionality on both aryl rings could increase the potency. As part of our evaluation process, we have also demonstrated that these compounds are capable of suppressing LPS-induced inflammatory response in both macrophage cells and a human whole blood *ex vivo* model.

Although the potency values of the compounds described herein are modest, it should be noted that they presumably function by disrupting the association of TLR4 and MD2.²³ Energetically, it is a challenging goal to compete with two protein binding partners and block their association with small molecule agents.^{15,41,42} The micromolar inhibitory activities observed with the β-amino alcohol derivatives are promising starting point for further drug development optimization.

It is anticipated that as improvements in potency, metabolic stability, and safety occur, these β-amino alcohol derivatives will serve as useful probes in studying TLR4-mediated inflammation and could pave the way for future antisepsis therapeutics.

EXPERIMENTAL SECTION

Secreted Nitric Oxide Assay. RAW264.7 cells were grown in RPMI supplemented with 10% FBS, penicillin–streptomycin, and L-glutamine.

RAW264.7 cells were then planted in 96-well plates at 100 000 cells per well and grown for 24 h in the medium described previously.^{43,44} After 24 h, the medium was removed and replaced with unsupplemented RPMI (Invitrogen, Carlsbad, CA). Lanes were doped with the TLR agonists and simultaneously doped with small molecule drugs as specified for each experiment. Plates were then incubated at 37 °C for 18–24 h. Following 18–24 h of incubation, 100 μL of medium was removed and added to flat black 96-well Microfluor plates (Thermo Scientific, Hudson, NH). An amount of 10 μL of 2,3-diaminonaphthalene (0.05 mg/mL in 0.62 M HCl) was added to each well and incubated for 15 min. Then 5 μL of 3 M NaOH was added to stop the reaction and the plate was read on a Beckman Coulter DTX880 reader with excitation set at 365 nm and emission analyzed at 450 nm. Nitrite concentration was determined from nitrite standard curve.

Trypan Blue Toxicity Assay. Human embryonic kidney 293 (HEK293) cells were stably transfected with TLR4 and necessary assembly and signaling proteins (MD2, CD-14, LPSBP, etc.). Cells were cultured in DMEM supplemented with 10% FBS, penicillin (100 U/mL), streptomycin (100 mg/mL), L-glutamine (2 mM), 1 mg/mL normocin (InvivoGen, San Diego, CA), and 2 units of HEK-Blue Selection solution (InvivoGen, San Diego, CA). Cells were implanted in 6 cm plates and grown to 65–85% confluency by incubating at 37 °C prior to drug treatment. On the day of treatment, the medium was removed from the 6 cm plate and replaced with CSF buffer supplemented with drug treatment. After 24 h of incubation at 37 °C, CSF was removed and cells were agitated with 1× trypsin and resuspended in fresh DMEM supplemented medium. After resuspension, a 100 μL sample was taken from each 6 cm plate, mixed gently with 100 μL of Trypan blue, and allowed to sit for 5 min. The ratio of blue stained cells to total cells was then quantified using a Bright Line 0.1 mm depth hemocytometer under a Nikon TMS light microscope.

Whole Blood Cytokine Release Assay. The following studies were approved by the regional ethics committee in Norway. Human whole blood was drawn from healthy individuals after giving their written consent. The whole blood model of sepsis has been described in detail previously.³⁸ Briefly, blood was drawn from healthy human donors into 4.5 mL cryotube vials (Nunc, Roskilde, Denmark) containing lepirudin (Refludan, Pharmion, Copenhagen, Denmark) in a final concentration of 50 μg/mL. Lepirudin is a highly specific thrombin inhibitor preventing coagulation only, not interfering with other biological activities. Small molecule drugs or PBS with Ca²⁺ and Mg²⁺ (Sigma, D8662) were administered to 1.8 mL cryotube vials prior to blood sampling. Immediately after the sample was obtained, blood was added to each of the respective tubes and preincubated with inhibitors at 37 °C for 5–10 min. Afterward they were supplied with 100 ng/mL phenol-extracted ultrapure LPS (upLPS) from *E. coli* 0111:B4 (InvivoGen, San Diego, CA, U.S.) or endotoxin-free PBS with Ca²⁺ and Mg²⁺. Samples were incubated, rotating at 37 °C for 2 h. Then ethylenediaminetetraacetic acid (EDTA) (Sigma) was added to a final concentration of 10 mM, and the samples were centrifuged 15 min at 3220g, 4 °C. Plasma was obtained and stored at –80 °C until further analysis.

Plasma levels of TNF-α, IL-8, and IL-6 were determined using singleplex Bio-plex cytokine kits from BioRad (Hercules, CA, U.S.). The analyses were performed according to the manufacturer's recommendations. The plasma cytokine concentration measured upon LPS stimulation in the absence of inhibitor was set to 100%. For statistical analyses, based on the data set of *n* = 3 (Figure 2A) or *n* = 9 (Figure 2B), a two-sided, paired Student's *t* test was performed based on single data points of % plasma cytokine levels.

Metabolic Stability. *Metabolic Stability in Human Liver Microsomes.* Compound **1j** (1 μM) with <0.25% DMSO was incubated at 37 °C in buffer with 0.5 mg/mL microsomal protein. The reaction was initiated by the addition of cofactors at five different time points (0, 10,

20, 30, and 60 min). A positive control (5 μM testosterone) was run in parallel with sampling at 1, 10, and 30 min. After the final time point, fluorimetry was used to confirm the addition of NADPH to the reaction mixture. LC–MS/MS was used to determine the peak area response ratio (peak area corresponding to **1j** divided by that of an internal standard) without running a standard curve. The in vitro intrinsic clearance $\text{CL}_{\text{int in vitro}} = k/P$ (mL/min \cdot mg protein) was determined, where k is the elimination rate constant (min^{-1}) and P is the protein concentration (mg/mL).

Metabolic Stability in Liver S9 Fractions. Compound **1j** (1 μM) in <0.25% DMSO was incubated at 37 $^{\circ}\text{C}$ in buffer with 1 mg/mL of pooled S9 protein from both rat and human and 1 mM NADPH, UDPGA, PAPS, and GSH. The reaction was initiated by the addition of cofactors at five different time points (0, 10, 20, 30, and 60 min). A positive control (20 μM testosterone and 20 μM 7-hydroxycoumarin) was run in parallel with sampling at 1, 10, 30, and 60 min. After the final time point, fluorimetry was used to confirm the addition of NADPH to the reaction mixture. LC–MS/MS was used to determine the peak area response ratio (peak area corresponding to **1j** divided by that of an internal standard) without running a standard curve. The in vitro intrinsic clearance $\text{CL}_{\text{int in vitro}} = k/P$ (mL/min \cdot mg protein) was determined, where k is the elimination rate constant (min^{-1}) and P is the protein concentration (mg/mL).

CYP IC₅₀ in Human Liver Microsomes. The IC₅₀ values of **1j** for five CYP enzymes (1A2, 2C9, 2C19, 2D6, and 3A4) were determined using a pool of mixed-gender human liver microsomes (minimum of 10 donors). Compound **1j** was incubated with pooled human liver microsomes (0.25 mg/mL) at 37 $^{\circ}\text{C}$ in the presence of phosphate buffer (100 mM, pH 7.4), MgCl_2 (5 mM), CYP-specific probe (at approximately K_m), and NADPH (1 mM) at eight concentrations (0–100 μM). After a period of incubation, the samples were treated by the addition of protein precipitation solvent and centrifuged. The CYP enzyme activities were measured by determining the formation of the CYP probe metabolites by LC–MS/MS. The individual CYP isoforms (specific probe/metabolite formed/known inhibitor used as the positive control) tested were the following: CYP 1A2 (phenacetin (150 μM)/acetaminophen/ α -naphthoflavone); CYP 2C9 (diclofenac (6 μM)/4'-OH diclofenac/sulfaphenazole); CYP 2C19 (S-mephenytoin (40 μM)/4'-OH mephenytoin/(+)-N-3-benzylrivanol); CYP 2D6 (bufuralol (7 μM)/1'-OH bufuralol/quinidine); CYP 3A4 (testosterone (75 μM)/6 β -OH testosterone/ketoconazole); CYP 3A4 (midazolam (1.4 μM)/1'-OH midazolam/ketoconazole). The IC₅₀ was estimated by fitting the experimental data to a sigmoidal model and nonlinear regression analysis using GraphPad Prism software.

Kinase Profiling. The kinase profiling was performed by Luceome Biotechnologies, Tucson, AZ. Compounds **1j** and **1s** were dissolved in DMSO and tested at concentrations of 28 and 16 μM , respectively. Each compound was first evaluated for false positive against split luciferase. If they did not inhibit luciferase control, then they were profiled in duplicate against the following kinases: AKT1, CAMK1, DDR2, GSK3 α , MARK1, MET, PAK1, PDGFRB, PIM1, PKC- γ , PKL4, and SRC using the protocol described by Ghosh and co-workers.⁴⁵ The percent inhibition and percent activity remaining was calculated using the following equations:

$$\% \text{ inhibition} = [(ALU_{\text{control}} - ALU_{\text{sample}}) / ALU_{\text{control}}] \times 100$$

$$\% \text{ activity remaining} = 100 - \% \text{ inhibition}$$

General Chemistry Methods. All reactions were run under an inert atmosphere of either N_2 or Ar gas. Reaction solvents were purchased anhydrous and of HPLC quality. All other reagents were purchased from Sigma Aldrich and used without further purification. Yields were calculated for material judged homogeneous by thin layer

chromatography (TLC) and nuclear magnetic resonance (NMR). TLC was performed on Merck Kieselgel 60 F₂₅₄ plates, eluting with the solvent indicated, visualized by a 254 nm UV lamp, and stained with an ethanolic solution of phosphomolybdic acid hydrate. Glassware for reactions was oven-dried at 125 $^{\circ}\text{C}$ prior to use. Column flash chromatography was performed using silica gel (SiO_2) Premium R₆, 60 \AA , 200 \times 400 mesh from Sorbent Technologies. Nuclear magnetic resonance spectra were acquired on a Bruker spectrometer (300 MHz for ^1H and 75 MHz for ^{13}C) or a Varian Inova-400 (400 MHz for ^1H and 100 MHz for ^{13}C). Chemical shifts for ^1H NMR spectra are reported in parts per million (ppm) and referenced to the signal of residual CDCl_3 at 7.26 ppm. Chemical shifts for ^{13}C NMR and DEPT spectra are reported in parts per million (ppm) and referenced to the center line of the residual CDCl_3 triplet at 77.23 ppm. Chemical shifts of the unprotonated carbons ("C") for DEPT spectra were obtained by comparison with the ^{13}C NMR spectrum. Enantiomeric excess was determined by chiral HPLC analysis using a Daicel Chiralcel AD-H silica column (length = 25 cm), eluting with a mobile phase of an indicated percentage of *i*-PrOH/hexanes with 0.1% Et_2NH and at a flow rate of 0.5 mL/min. Retention times for the major and minor enantiomers were detected with Shimadzu SPD-6A UV spectrometric detector at 254 nm. Optical rotations were obtained on a Jasco P1038 polarimeter (Na D line) using a microcell with a 1 dm path length. Specific rotations ($[\alpha]_D^{20}$, unit, $\text{deg cm}^2/\text{g}$) are based on the equation $\alpha = (100\alpha)/(lc)$ and are reported as unitless numbers where the concentration c is in g/100 mL and the path length l is in decimeters. High resolution mass spectrometry data were obtained at the mass spectrometer facility of the University of Colorado Boulder, Department of Chemistry and Biochemistry, on an ESI-qTOF-MS (electrospray triple quadrupole time-of-flight mass spectrometry) spectrometer from Applied Biosystems, PE SCIEX/ABI API QSTAR Pulsar i Hybrid LC/MS/MS. All compounds tested have a purity of $\geq 95\%$ as determined by TLC, NMR, HRMS, and chiral HPLC for chiral compounds. Compounds were named using ChemBioDraw Ultra 11.0.

General Synthetic Procedures for Racemic Epoxides of Type 2. 2-((4-Chlorophenoxy)methyl)oxirane (2d). Into a 50 mL round-bottom flask, (4-chloro)phenol (1.00 g, 7.78 mmol, 1 equiv) was taken up into acetone (20 mL, 0.4 M), and K_2CO_3 (3.22 g, 23.3 mmol, 3 equiv) and epichlorohydrin (2.34 mL, 31.1 mmol, 4 equiv) were added consecutively. The reaction mixture was set to stir at reflux for 24 h. At this time an additional 4 equiv of epichlorohydrin was added and the solution was allowed to stir at reflux for an additional 24 h.

The mixture was cooled to room temperature, and the solids were filtered off. The solvent was removed under reduced pressure and the resulting oil was taken up in toluene (20 mL). The organic layer was washed with H_2O (1 \times 20 mL), 1 M aqueous NaOH solution (1 \times 20 mL), and H_2O (1 \times 30 mL). The organic layer was dried over Na_2SO_4 , filtered, and the solvent was removed under reduced pressure. The resulting yellow oil was purified via flash SiO_2 chromatography (4.5 cm \times 5 cm, 10% EtOAc/hexanes) to yield the desired epoxide **2d** as a yellow oil (1.19 g, 84%); $R_f = 0.22$ (10% EtOAc/hexanes); ^1H NMR (400 MHz, CDCl_3) δ 7.25–7.19 (m, 2H), 7.25–7.19 (m, 2H), 6.87–6.81 (m, 2H), 6.86–6.81 (m, 2H), 4.20 (dd, $J = 2.95, 11.03$ Hz, 1H), 3.88 (dd, $J = 5.82, 11.03$ Hz, 1H), 3.33 (ddt, $J = 2.81, 2.81, 4.13, 5.72$ Hz, 1H), 2.89 (dd, $J = 4.18, 4.86$ Hz, 1H), 2.73 (dd, $J = 2.66, 4.90$ Hz, 1H); ^{13}C NMR (101 MHz, CDCl_3) δ 157.20 (C), 129.49 (CH), 126.19 (C), 116.04 (CH), 69.17 (CH_2), 50.17 (CH), 44.70 (CH_2); HRMS (ESI⁺), calcd $\text{C}_9\text{H}_9\text{ClO}_2\text{Li}$ ($M + \text{Li}^+$) = 191.0445, found = 191.0440.

General Synthetic Procedure for the Pyrazole Fragments of Type 6. 1-(3-Chlorobenzyl)-3,5-dimethyl-1H-pyrazole (6c). In a 25 mL round-bottom flask with DMSO (14.5 mL), KOH (0.88 g, 15.6 mmol, 1.5 equiv) and 3,5-dimethylpyrazole (1.00 g, 10.4 mmol, 1 equiv) were combined and set to stir at room temperature. This mixture

was then heated at 80 °C for 1 h. The mixture was then cooled to room temperature, and 3-chlorobenzyl chloride (1.32 mL, 10.4 mmol, 1 equiv) was added. The reaction mixture was allowed to stir for an additional 2 h.

Upon completion, the mixture was poured into H₂O (50 mL) and the solution was extracted with CHCl₃ (4 × 50 mL). The resulting organic layers were washed with H₂O (4 × 100 mL) to remove DMSO, dried over Na₂SO₄, filtered, and concentrated under reduced pressure. The resulting material was purified via flash SiO₂ column chromatography (5.5 cm × 5 cm, 5% EtOAc/hexanes) to yield the desired pyrazole **6c** as a yellow oil (2.11 g, 92%); *R*_f = 0.139 (10% EtOAc/hexanes); ¹H NMR (300 MHz, CDCl₃) δ 7.23–7.18 (m, 2H), 7.05–7.01 (m, 1H), 6.96–6.89 (m, 1H), 5.85 (s, 1H), 5.16 (s, 2H), 2.24 (s, 3H), 2.14 (s, 3H); ¹³C NMR (75 MHz, CDCl₃) δ 148.06 (C), 139.62 (C), 139.34 (C), 134.78 (C), 130.13 (CH), 127.83 (CH), 126.81 (CH), 124.85 (CH), 105.93 (CH), 52.06 (CH₂), 13.69 (CH₃), 11.24 (CH₃); HRMS (ESI⁺), calcd C₁₂H₁₃ClN₂Na (M + Na⁺) = 243.0659, found = 243.0652.

General Synthetic Procedure for Methyl Amine Fragment of Type 3. 1-(1-(3-Chlorobenzyl)-3,5-dimethyl-1H-pyrazol-4-yl)-N-methylmethanamine (3c). In a 25 mL round-bottom flask, methylamine–HCl (0.92 g, 13.6 mmol, 3 equiv) and paraformaldehyde (0.82 g, 27.2 mmol, 6 equiv) were combined in EtOH (9 mL). This solution was stirred for 2 h at 60 °C. At this point, the pyrazole derivative 1-(3-chlorobenzyl)-3,5-dimethyl-1H-pyrazole (**6c**) (1.00 g, 4.5 mmol, 1 equiv) was added, and the mixture was heated to 75 °C and stirred for 21 h.

Upon completion, the mixture was cooled to room temperature and the solvent was removed under reduced pressure. The resulting oil was taken up into 50 mL of CHCl₃ and washed with a saturated aqueous solution of NaHCO₃ (1 × 20 mL). The resulting aqueous layer was then extracted with CHCl₃ (3 × 30 mL) and then dried over Na₂SO₄, filtered, and concentrated under reduced pressure. The resulting yellow oil was purified via flash SiO₂ chromatography (5 cm × 4 cm, 40% EtOAc/hexanes with 2% Et₃N) to yield the desired methylamine **3c** as a yellow oil (0.467 g, 40%); *R*_f = 0.09 (60% EtOAc/hexanes with 2% Et₃N); ¹H NMR (300 MHz, CDCl₃) δ 7.23–7.18 (m, 2H), 7.01–6.96 (m, 1H), 6.95–6.88 (m, 1H), 5.18 (s, 2H), 3.27 (s, 2H), 2.87 (s, 1H), 2.23 (s, 3H), 2.12 (s, 3H), 2.11 (s, 3H); ¹³C NMR (75 MHz, CDCl₃) δ 147.92 (C), 139.82 (C), 137.98 (C), 134.82 (C), 130.13 (CH), 127.81 (CH), 126.75 (CH), 124.79 (CH), 114.56 (C), 52.21 (CH₂), 49.02 (CH₂), 40.64 (CH₃), 12.28 (CH₃), 9.89 (CH₃); HRMS (ESI⁺), calcd C₁₄H₁₉ClN₃ (M + H⁺) = 264.1262, found = 264.1263.

Methods for the Synthesis of β-Hydroxyamide Compounds of Type 1. *Method A:* 1-(((1-Benzyl-3,5-dimethyl-1H-pyrazol-4-yl)methyl)(methyl)amino)-3-phenoxypropan-2-ol (**1a**). To a 10 mL round-bottom flask, 3.33 mL of absolute EtOH was added. To this the amine, 1-(1-benzyl-3,5-dimethyl-1H-pyrazol-4-yl)-N-methylmethanamine (**3a**) (0.17 g, 0.73 mmol, 1.1 equiv) and the commercially available epoxide **2a** (0.10 g, 0.66 mmol, 1.0 equiv) were combined. The reaction mixture was set to stir for 22 h at reflux.

When the reaction was complete, the mixture was cooled to room temperature and the solvent was removed under reduced pressure. The resulting oil was taken up in CHCl₃ (30 mL) and washed with a saturated aqueous solution of NaHCO₃ (1 × 20 mL). The resulting aqueous layer was extracted with CHCl₃ (3 × 30 mL). The combined organic layers were then dried over Na₂SO₄, filtered, and the solvent was removed under reduced pressure. The resulting oil was purified via flash SiO₂ column chromatography (3.0 cm × 4.0 cm, 50% EtOAc/hexanes with 2% Et₃N) to yield the desired alcohol **1a** as a clear oil (0.13 g, 50%); *R*_f = 0.46 (50% EtOAc/hexanes with 2% Et₃N); ¹H NMR (300 MHz, CDCl₃) δ 7.33–7.19 (m, 4H), 7.08–7.00 (m, 2H), 6.98–6.86 (m, 4H), 5.21 (s, 2H), 4.16–4.01 (m, 2H), 3.95 (s, 2H), 3.53 (br s, 1H), 3.37 (ABq, *J* = 12.90 Hz, Δ*v* = 45.41 Hz, 2H), 2.60 (dd, *J* = 9.41, 12.24 Hz,

1H), 2.48 (dd, *J* = 4.77, 11.80 Hz, 1H), 2.25 (s, 1H), 2.23 (s, 1H), 2.11 (s, 1H); ¹³C NMR (75 MHz, CDCl₃) δ 158.96 (C), 147.50 (C), 138.18 (C), 137.54 (C), 129.65 (CH), 128.93 (CH), 127.67 (CH), 126.69 (CH), 121.14 (CH), 114.73 (CH), 113.62 (C), 70.53 (CH₂), 66.29 (CH), 59.58 (CH₂), 53.02 (CH₂), 51.73 (CH₂), 42.05 (CH₃), 12.35 (CH₃), 10.05 (CH₃); HRMS (ESI⁺), calcd C₂₃H₂₉N₃O₂Na (M + Na⁺) = 402.2152, found = 402.2168.

Method B: 1-(((1-(2-Chlorobenzyl)-3,5-dimethyl-1H-pyrazol-4-yl)methyl)(methyl)amino)-3-(4-ethoxyphenoxy)propan-2-ol (**1j**). Into a 25 mL round-bottom flask, the epoxide 2-((4-ethoxyphenoxy)methyl)oxirane (**2b**) (0.300 g, 1.54 mmol, 1 equiv), amine 1-(1-(2-chlorobenzyl)-3,5-dimethyl-1H-pyrazol-4-yl)-N-methylmethanamine (**3b**) (0.45 g, 1.70 mmol, 1.1 equiv), and K₂CO₃ (0.23 g, 1.62 mmol, 1 equiv) were combined in acetonitrile (5.7 mL, 0.27 M). This solution was heated to reflux for 24 h, at which time the reaction was complete. The solvent was removed under reduced pressure, and the resulting yellow oil was taken up into 10 mL of CHCl₃ and partitioned into a saturated aqueous solution of NaHCO₃ (10 mL) and CHCl₃ (10 mL). The layers were separated, and the aqueous layer was back-extracted with CHCl₃ (4 × 30 mL). The organic layers were combined and dried over Na₂SO₄, filtered, and the solvent was removed under reduced pressure.

The resulting yellow oil was purified via flash SiO₂ column chromatography (2.5 cm × 4 cm, 40% EtOAc/hexanes with 2% Et₃N) to yield the desired alcohol **1j** as a white solid (0.612 g, 87%); *R*_f = 0.300 (60% EtOAc/hexanes with 2% Et₃N); ¹H NMR (300 MHz, CDCl₃) δ 7.38–7.33 (m, 1H), 7.22–7.09 (m, 2H), 6.87–6.78 (m, 4H), 6.51–6.47 (m, 1H), 5.30 (s, 2H), 4.12–4.03 (m, 1H), 3.98 (q, *J* = 6.96, 6.98, 6.98 Hz, 2H), 3.90 (d, *J* = 4.98 Hz, 2H), 3.40 (ABq, *J* = 13.19, Δ*v* = 47.60 Hz, 2H), 2.61 (dd, *J* = 9.58, 12.25 Hz, 1H), 2.47 (dd, *J* = 4.18, 12.24 Hz, 1H), 2.26 (s, 3H), 2.25 (s, 2H), 2.12 (s, 2H), 1.39 (t, *J* = 6.99 Hz, 3H); ¹³C NMR (75 MHz, CDCl₃) δ 153.52 (C), 153.09 (C), 148.08 (C), 138.70 (C), 135.36 (C), 131.97 (C), 129.47 (CH), 128.82 (CH), 127.63 (CH), 127.53 (CH), 115.68 (CH), 115.58 (CH), 113.66 (C), 71.30 (CH₂), 66.40 (CH), 64.20 (CH₂), 59.57 (CH₂), 51.74 (CH₂), 50.33 (CH₂), 42.12 (CH₃), 15.16 (CH₃), 12.40 (CH₃), 9.86 (CH₃); HRMS (ESI⁺), calcd C₂₅H₃₃ClN₃O₃ (M + H⁺) = 458.2205, found = 458.2199.

Method C: (S)-1-(((1-(2-Chlorobenzyl)-3,5-dimethyl-1H-pyrazol-4-yl)methyl)(methyl)amino)-3-(4-ethoxyphenoxy)propan-2-ol (**1l**). Into a 5 mL reaction vial, the epoxide (S)-2-((4-ethoxyphenoxy)methyl)oxirane (**2h**) (0.017 g, 0.087 mmol, 1 equiv) and the amine, 1-(1-(2-chlorobenzyl)-3,5-dimethyl-1H-pyrazol-4-yl)-N-methylmethanamine (**3b**) (0.023 g, 0.087 mmol, 1.1 equiv) were taken up into toluene (0.3 mL, 0.3 M) and set to reflux for 48 h.

The reaction mixture was cooled to room temperature, transferred to a 25 mL round-bottom flask, and the solvent was removed under reduced pressure. The resulting orange oil was purified via flash SiO₂ column chromatography (1.5 cm × 4 cm, 60% EtOAc/hexanes with 2% Et₃N) to yield the desired chiral alcohol (**1l**) as a clear oil (0.025 g, 63%); *R*_f = 0.210 (50% EtOAc/hexanes with 2% Et₃N). Assay of enantiomeric excess: HPLC (Chiralcel AD 25 cm column, 20% *i*-PrOH/hexanes with 0.1% Et₂NH; 1.0 mL/min) *t*_R (major) = 4.56 min, *t*_R (minor) = 5.7 min; >96% ee; [α]_D²⁵ = -15.06 (c 0.649, CHCl₃); ¹H NMR (400 MHz, CDCl₃) δ 7.35 (dd, *J* = 1.42, 7.79 Hz, 1H), 7.15 (dtd, *J* = 1.55, 7.43, 7.45, 20.61 Hz, 1H), 6.85–6.79 (m, 2H), 6.51–6.43 (m, 1H), 5.30 (s, 1H), 4.08 (dddd, *J* = 5.33, 5.33, 5.33, 9.28 Hz, 1H), 3.97 (q, *J* = 6.97, 6.98, 6.98 Hz, 1H), 3.90 (d, *J* = 4.96 Hz, 1H), 3.42 (s, 1H), 3.40 (ABq, *J* = 13.19 Hz, Δ*v* = 63.80 Hz, 1H), 2.61 (dd, *J* = 9.70, 12.18 Hz, 1H), 2.47 (dd, *J* = 4.13, 12.24 Hz, 1H), 2.26 (s, 1H), 2.25 (s, 1H), 2.12 (s, 1H); ¹³C NMR (101 MHz, CDCl₃) δ 153.45 (C), 153.03 (C), 148.05 (C), 138.68 (C), 135.32 (C), 131.91 (C), 129.43 (CH), 128.79 (CH), 127.55 (CH), 127.51 (CH), 115.61 (CH), 115.50 (CH), 113.70 (C), 71.22 (CH₂), 66.33 (CH), 64.13 (CH₂), 59.50 (CH₂), 51.69 (CH₂), 50.30 (CH₂),

42.07 (CH₃), 15.15 (CH₃), 12.39 (CH₃), 9.84 (CH₃); HRMS (ESI⁺), calcd C₂₅H₃₃ClN₂O₃ (M + H⁺) = 458.2205, found = 458.2191.

Method D: 1-(4-(Allyloxy)phenoxy)-3-(((3,5-dimethyl-1-(2-vinylbenzyl)-1H-pyrazol-4-yl)methyl)(methyl)amino)propan-2-ol (**1q**). Into a 5 mL Biotage microwave tube, the epoxide 2-((4-(allyloxy)phenoxy)-methyl)oxirane (**2c**) (0.038 g, 0.182 mmol, 1 equiv) and the amine 1-(3,5-dimethyl-1-(2-vinylbenzyl)-1H-pyrazol-4-yl)-N-methylmethanamine (**3f**) (0.051 g, 0.20 mmol, 1.1 equiv) were combined in absolute ethanol (0.455 mL). The tube was then sealed with the appropriate crimp cap and the tube placed into the microwave. After a total of 15 min (200 W, 140 °C, 4–5 bar) the reaction was complete.

The reaction mixture was transferred to a round-bottom with ethyl acetate, and the solvent was removed under reduced pressure. The resulting oil was diluted with CHCl₃ (20 mL) and washed with a saturated aqueous solution of NaHCO₃ (1 × 10 mL). The aqueous layer was extracted with CHCl₃ (2 × 20 mL), and the combined organic layers were dried over Na₂SO₄, filtered, and the solvent was removed under reduced pressure. The resulting material was purified via flash SiO₂ column chromatography (1.5 cm × 6.5 cm, 60% EtOAc/hexanes with 2% Et₃N) to yield the desired alcohol **1q** (0.072 g, 86%); *R*_f = 0.25 (60% EtOAc/hexanes with 2% Et₃N); ¹H NMR (300 MHz, CDCl₃) δ 7.46 (dd, *J* = 1.46, 7.61 Hz, 1H), 7.25–7.10 (m, 2H), 6.96 (dd, *J* = 10.95, 17.29 Hz, 1H), 6.83 (s, 4H), 6.47 (dd, *J* = 0.88, 7.59 Hz, 1H), 6.12–5.97 (m, 1H), 5.65 (dd, *J* = 1.37, 17.27 Hz, 1H), 5.39 (d, *J* = 1.33 Hz, 1H), 5.37–5.35 (m, 1H), 5.33 (dq, *J* = 1.42, 1.53, 1.53, 51.83 Hz, 1H), 5.30–5.27 (m, 2H), 4.48 (dt, *J* = 1.52, 1.52, 5.31 Hz, 2H), 4.14–4.02 (m, 1H), 3.90 (d, *J* = 5.03 Hz, 2H), 3.39 (ABq, *J* = 13.20 Hz, Δ*v* = 47.40 Hz, 2H), 3.27 (br s, 1H), 2.60 (dd, *J* = 9.53, 12.19 Hz, 1H), 2.47 (dd, *J* = 4.21, 12.25 Hz, 1H), 2.25 (s, 2H), 2.24 (s, 2H), 2.07 (s, 2H); ¹³C NMR (75 MHz, CDCl₃) δ 153.29 (C), 153.14 (C), 147.68 (C), 138.56 (C), 135.92 (C), 134.59 (C), 133.76 (CH), 133.74 (CH), 128.44 (CH), 127.73 (CH), 126.33 (CH), 126.30 (CH), 117.71 (CH₂), 117.38 (CH₂), 115.86 (CH), 115.63 (CH), 113.60 (C), 71.28 (CH₂), 69.67 (CH₂), 66.36 (CH), 59.54 (CH₂), 51.72 (CH₂), 50.70 (CH₂), 42.06 (CH₃), 12.38 (CH₃), 9.97 (CH₃); HRMS (ESI⁺), calcd C₂₈H₃₆N₃O₃ (M + H⁺) = 462.2751 found = 462.2750.

Method E: 1-(((1-(2-Chlorobenzyl)-3,5-dimethyl-1H-pyrazol-4-yl)-methyl)(methyl)amino)-3-(4-chlorophenoxy)propan-2-ol (**1s**). Into a 5 mL Biotage microwave tube the epoxide 2-((4-chlorophenoxy)-methyl)oxirane (**2d**) (0.05 g, 0.27 mmol, 1 equiv), the amine 1-(1-(2-chlorobenzyl)-3,5-dimethyl-1H-pyrazol-4-yl)-N-methylmethanamine (**3b**) (0.078 g, 0.300 mmol, 1.1 equiv), and K₂CO₃ (0.036 g, 0.271 mmol, 1 equiv) were all taken up in acetonitrile (1 mL, 0.27 M). The tube was then sealed with the appropriate crimp cap and the tube placed into the microwave. After a total of 50 min (200 W, 180 °C, 9 bar) the reaction was complete. The reaction tube was cooled to room temperature, the cap was removed, and the reaction mixture was transferred to a 15 mL round-bottom flask with EtOAc. The solvent was removed under reduced pressure, and the resulting oil was diluted with CHCl₃ (10 mL). This solution was partitioned into a separatory funnel containing a 1:1 solution of CHCl₃ and a saturated aqueous solution of NaHCO₃ (10 mL each). The layers were separated, and the organic layer was extracted with CHCl₃ (2 × 10 mL). The combined organic layers were dried over Na₂SO₄, filtered, and the solvent was removed under reduced pressure to yield an orange oil.

This oil was purified via flash SiO₂ column chromatography (2.5 cm × 4 cm, 60% EtOAc/hexanes with 2% Et₃N) to yield the desired alcohol (**1s**) as a yellow oil (0.121 g, quant); *R*_f = 0.25 (60% EtOAc/hexanes with 2% Et₃N); ¹H NMR (300 MHz, CDCl₃) δ 7.33 (dd, *J* = 1.44, 7.71 Hz, 1H), 7.23–7.16 (m, 2H), 7.17–7.06 (m, 2H), 6.85–6.74 (m, 2H), 6.48 (dd, *J* = 1.60, 7.51 Hz, 1H), 5.28 (s, 2H), 4.18–3.96 (m, 1H), 3.97–3.79 (m, 2H), 3.38 (ABq, *J* = 13.18 Hz, Δ*v* = 45.8 Hz, 3H), 2.58 (dd, *J* = 9.54, 12.17 Hz, 1H), 2.45 (dd, *J* = 4.29, 12.23 Hz, 1H), 2.24 (s, 3H), 2.24 (s, 3H), 2.10 (s, 3H); ¹³C NMR (101 MHz, CDCl₃) δ 157.55

(C), 148.02 (C), 138.66 (C), 135.29 (C), 132.07 (C), 129.67 (CH), 128.82 (CH), 127.56 (CH), 115.97 (C), 113.65 (C), 70.84 (CH₂), 66.15 (CH), 59.26 (CH₂), 51.70 (CH₂), 50.59 (CH₂), 42.07 (CH₃), 12.39 (CH₃), 9.74 (CH₃); HRMS (ESI⁺), calcd C₂₃H₂₈Cl₂N₃O₂Na (M + H⁺) = 448.1538, found = 448.1553.

N-((1-(2-Chlorobenzyl)-3,5-dimethyl-1H-pyrazol-4-yl)-methyl)-3-(4-ethoxyphenoxy)-2-methoxy-N-methylpropan-1-amine (7). Into a 10 mL round-bottom flask, the alcohol 1-(((1-(2-chlorobenzyl)-3,5-dimethyl-1H-pyrazol-4-yl)methyl)(methyl)amino)-3-(4-ethoxyphenoxy)propan-2-ol (**1j**) (0.020 g, 0.044 mmol, 1 equiv) was taken up in THF (2.2 mL). To this, NaH (60%, 0.023 g, 0.96 mmol, 22 equiv) was added, and the mixture was stirred for 10 min. MeI (0.08 mL, 1.3 mmol, 30 equiv) was added dropwise. The solution was allowed to stir at room temperature for 30 min, at which time, it appeared complete by TLC. The reaction mixture was quenched by the slow addition of 2 mL of a saturated aqueous solution of NH₄Cl. Once the effervescence ceased (about 1 h) the mixture was diluted with ether, and the layers were separated. The aqueous layer was back-extracted with ether (1 × 20 mL) and then CH₂Cl₂ 2 × 20 mL. The combined organic layers were dried over Na₂SO₄, filtered, and the solvent was removed under reduced pressure. The resulting dark brown oil was purified via flash SiO₂ column chromatography (2 cm × 3 cm, dry loaded on SiO₂, 40% EtOAc/hexanes with 2% Et₃N) to yield the desired methyl ether (**7**) as a clear oil (0.0078 g, 37%); *R*_f = 0.212 (60% EtOAc/hexanes with 2% Et₃N); ¹H NMR (400 MHz, CDCl₃) δ 7.34 (dd, *J* = 1.25, 7.87 Hz, 1H), 7.17 (td, *J* = 1.77, 7.66, 7.87 Hz, 1H), 7.10 (td, *J* = 1.38, 7.45, 7.53 Hz, 1H), 6.83–6.76 (m, 4H), 6.47 (d, *J* = 6.15 Hz, 1H), 5.25 (s, 2H), 4.03 (dd, *J* = 3.50, 9.98 Hz, 1H), 3.97 (q, *J* = 6.97, 6.98, 6.98 Hz, 2H), 3.87 (dd, *J* = 5.51, 10.00 Hz, 1H), 3.48 (s, 3H), 3.39–3.25 (m, 2H), 2.64–2.56 (m, 1H), 2.53–2.45 (m, 1H), 2.24 (s, 3H), 2.23 (s, 3H), 2.07 (s, 3H), 1.38 (t, *J* = 6.99 Hz, 3H); ¹³C NMR (101 MHz, CDCl₃) δ 153.34, 153.15, 148.16, 135.47, 131.91, 129.42, 128.75, 127.58, 127.47, 115.56, 115.49, 69.51, 64.15, 57.99, 57.40, 52.32, 50.21, 43.19, 29.92, 15.17, 12.33, 9.76; HRMS (ESI⁺), calcd C₂₆H₃₅ClN₃O₃ (M + H⁺) = 472.2382, found = 472.2361.

Macrocycle 8. To a 50 mL round-bottom flask, the β-amino alcohol **1q** (0.05 g, 0.11 mmol, 1 equiv) was dissolved in toluene (21 mL). The solution was degassed. Grubbs II catalyst (0.0009 g, 0.011 mmol, 0.1 equiv) was added, and reaction mixture was degassed again. This mixture was stirred for 7 h at 110 °C. At this time, the mixture was cooled to room temperature and the solvent was removed under reduced pressure. The dark brown oil was purified via flash SiO₂ column chromatography (1.5 cm × 7.0 cm, 60% EtOAc/hexanes with 2% Et₃N) to yield **8** as a yellow oil (0.024 g, 52%); *R*_f = 0.38 (60% EtOAc/hexanes with 2% Et₃N); ¹H NMR (300 MHz, CDCl₃) δ 7.20–7.08 (m, 4H), 6.96–6.88 (m, 2H), 6.84 (d, *J* = 6.65 Hz, 1H), 6.74 (d, *J* = 5.27 Hz, 1H), 6.74–6.69 (m, 2H), 5.77 (dt, *J* = 5.83, 5.83, 16.01 Hz, 1H), 4.86 (d, *J* = 5.66 Hz, 2H), 4.62 (ABq, *J* = 16.50 Hz, Δ*v* = 61.90 Hz, 2H), 3.98 (d, *J* = 7.24 Hz, 1H), 3.71–3.58 (m, 2H), 3.38 (d, *J* = 13.29 Hz, 1H), 3.34–3.19 (m, 2H), 2.56 (dd, *J* = 6.61, 12.46 Hz, 1H), 2.45 (s, 3H), 2.22 (s, 3H), 1.34 (s, 3H); ¹³C NMR (75 MHz, CDCl₃) δ 155.82, 153.37, 151.17, 147.10, 135.73, 134.78, 133.47, 130.00, 128.32, 128.23, 127.45, 127.08, 126.93, 119.18, 115.18, 69.31, 68.63, 66.64, 56.95, 52.03, 50.58, 12.13, 9.49; HRMS (ESI⁺) = calcd C₂₆H₃₂N₃O₃ (M + H⁺) = 434.2438, found = 434.2423.

Formation of β-Hydroxyamine HCl Salts. If required, the free bases of the following compounds were made into the HCl salts via the following procedure. The compound was dissolved in 0.5 M Et₂O. To this solution, an equal volume of 2 M HCl in Et₂O was added dropwise until the HCl salt precipitated out of solution. This mixture was allowed to stir for an additional 10 min. Then the solvent was evaporated off using a stream of N₂ gas. The HCl salt was then dried on high vacuum overnight and stored at room temperature over Dryrite.

■ ASSOCIATED CONTENT

S Supporting Information. Experimental data for all remaining compounds and additional biological results. This material is available free of charge via the Internet at <http://pubs.acs.org>.

■ AUTHOR INFORMATION

Corresponding Author

*Phone: +1-303-492-6786. Fax: +1-303-492-5894. E-mail: hang.yin@colorado.edu.

Author Contributions

[†]These authors contributed equally to this work and should be considered co-first-authors.

■ ACKNOWLEDGMENT

We thank the National Institutes of Health (Grants DA026950, DA025740, NS067425, RR025780, and DA029119) for financial support of this work. K.C. thanks the China Scholarship Council for a joint PhD scholarship (Grant No. 2009619072). Funding for M.N.P. was supplied by CU Undergraduate Research Opportunities Program and HHMI Biosciences. We thank Dr. Jonel Saludes, Dr. Peter Brown, and Dr. Greg Miknis for their suggestions for the manuscript. We thank Sara K. Coulup for synthetic assistance.

■ ABBREVIATIONS USED

AKT1, RAC- α serine/threonine-protein kinase; BBB, blood-brain barrier; CAMK1, calcium/calmodulin-dependent protein kinase type 1; CSF, cerebrospinal fluid; CD14, cluster of differentiation 14; CYP 450, cytochrome P450; DDR2, discoidin domain-containing receptor 2; DMEM, Dulbecco's modified Eagle medium; DMSO, dimethylsulfoxide; FBS, fetal bovine serum; GSK3 α , glycogen synthase kinase-3 α ; HEK293, human embryonic kidney 293 cells; IL-1, interleukin 1; IL-1 β , interleukin 1 β ; IL-6, interleukin 6; LPS, lipopolysaccharide; MARK1, MAP/microtubule affinity-regulating kinase 1; MeCN, acetonitrile; MD2, myeloid differentiation factor 2; NADPH, nicotinamide adenine dinucleotide phosphate; NF- κ B, nuclear factor κ B; NMR, nuclear magnetic resonance; NO, nitric oxide; PAPS, 3'-phosphoadenosine 5'-phosphosulfate; GSH, glutathione; PAK1, P21/Cdc42/Rac1-activated kinase 1; PDGF β , platelet-derived growth factor- β ; PBS, phosphate buffered saline; PIM1, proto-oncogene serine/threonine-protein kinase; PKC- γ , protein kinase γ ; PLK4, polo-like kinase 4; PPTS, pyridinium *p*-toluenesulfonate; RPMI, Roswell Park Memorial Institute; SRC, sarcoma kinase; TLC, thin layer chromatography; TLR-4, Toll-like receptor 4; TNF- α , tumor necrosis factor- α ; UDPGA, uridine 5'-diphosphoglucuronosyltransferase

■ REFERENCES

(1) Takeda, K.; Akira, S. Toll-like receptors in innate immunity. *Int. Immunol.* **2005**, *17*, 1–14.
(2) Fitzgerald, K. A.; Rowe, D. C.; Golenbock, D. T. Endotoxin recognition and signal transduction by the TLR4/MD2-complex. *Microbes Infect.* **2004**, *6*, 1361–1367.
(3) Park, B. S.; Song, D. H.; Kim, H. M.; Choi, B. S.; Lee, H.; Lee, J. O. The structural basis of lipopolysaccharide recognition by the TLR4-MD-2 complex. *Nature* **2009**, *458*, 1191–1195.

(4) Matzinger, P. The danger model: a renewed sense of self. *Science* **2002**, *296*, 301–305.
(5) Lehnardt, S.; Massillon, L.; Follett, P.; Jensen, F. E.; Ratan, R.; Rosenberg, P. A.; Volpe, J. J.; Vartanian, T. Activation of innate immunity in the CNS triggers neurodegeneration through a Toll-like receptor 4-dependent pathway. *Proc. Natl. Acad. Sci. U.S.A.* **2003**, *100*, 8514–8519.
(6) Peri, F.; Piazza, M.; Calabrese, V.; Damore, G.; Cighetti, R. Exploring the LPS/TLR4 signal pathway with small molecules. *Biochem. Soc. Trans.* **2010**, *38*, 1390–1395.
(7) Wittebole, X.; Castanares-Zapatero, D.; Laterre, P. F. Toll-like receptor 4 modulation as a strategy to treat sepsis. *Mediators Inflammation* **2010**, *2010*, 568396.
(8) Guo, L. H.; Schluesener, H. J. The innate immunity of the central nervous system in chronic pain: the role of Toll-like receptors. *Cell. Mol. Life Sci.* **2007**, *64*, 1128–1136.
(9) Tanga, F. Y.; Nutile-McMenemy, N.; DeLeo, J. A. The CNS role of Toll-like receptor 4 in innate neuroimmunity and painful neuropathy. *Proc. Natl. Acad. Sci. U.S.A.* **2005**, *102*, 5856–5861.
(10) Leon, C. G.; Tory, R.; Jia, J.; Sivak, O.; Wasan, K. M. Discovery and development of Toll-like receptor 4 (TLR4) antagonists: a new paradigm for treating sepsis and other diseases. *Pharm. Res.* **2008**, *25*, 1751–1761.
(11) Qu, J.; Zhang, J.; Pan, J.; He, L.; Ou, Z.; Zhang, X.; Chen, X. Endotoxin tolerance inhibits lipopolysaccharide-initiated acute pulmonary inflammation and lung injury in rats by the mechanism of nuclear factor-kappaB. *Scand. J. Immunol.* **2003**, *58*, 613–619.
(12) Johnson, D. A. Synthetic TLR4-active glycolipids as vaccine adjuvants and stand-alone immunotherapeutics. *Curr. Top. Med. Chem.* **2008**, *8*, 64–79.
(13) Meng, J.; Lien, E.; Golenbock, D. T. MD-2-mediated ionic interactions between lipid A and TLR4 are essential for receptor activation. *J. Biol. Chem.* **2010**, *285*, 8695–8702.
(14) Lipinski, C. A.; Lombardo, F.; Dominy, B. W.; Feeney, P. J. Experimental and computational approaches to estimate solubility and permeability in drug discovery and development settings. *Adv. Drug Delivery Rev.* **2001**, *46*, 3–26.
(15) Yin, H.; Hamilton, A. D. Strategies for targeting protein-protein interactions with synthetic agents. *Angew. Chem., Int. Ed.* **2005**, *44*, 4130–4163.
(16) Park, S. J.; Kang, S. H.; Kang, Y. K.; Eom, Y. B.; Koh, K. O.; Kim, D. Y.; Youn, H. S. Inhibition of homodimerization of Toll-like receptor 4 by 4-oxo-4-(2-oxo-oxazolidin-3-yl)-but-2-enoic acid ethyl ester. *Int. Immunopharmacol.* **2011**, *11*, 19–22.
(17) Jin, G. H.; Li, H.; An, S.; Ryu, J. H.; Jeon, R. Design, synthesis and activity of benzothiazole-based inhibitors of NO production in LPS-activated macrophages. *Bioorg. Med. Chem. Lett.* **2010**, *20*, 6199–6202.
(18) Kawamoto, T.; Ii, M.; Kitazaki, T.; Iizawa, Y.; Kimura, H. TAK-242 selectively suppresses Toll-like receptor 4-signaling mediated by the intracellular domain. *Eur. J. Pharmacol.* **2008**, *584*, 40–48.
(19) Takashima, K.; Matsunaga, N.; Yoshimatsu, M.; Hazeki, K.; Kaisho, T.; Uekata, M.; Hazeki, O.; Akira, S.; Iizawa, Y.; Ii, M. Analysis of binding site for the novel small-molecule TLR4 signal transduction inhibitor TAK-242 and its therapeutic effect on mouse sepsis model. *Br. J. Pharmacol.* **2009**, *157*, 1250–1262.
(20) Rice, T. W.; Wheeler, A. P.; Bernard, G. R.; Vincent, J. L.; Angus, D. C.; Aikawa, N.; Demeyer, I.; Sainati, S.; Amlot, N.; Cao, C.; Ii, M.; Matsuda, H.; Mourii, K.; Cohen, J. A randomized, double-blind, placebo-controlled trial of TAK-242 for the treatment of severe sepsis. *Crit. Care Med.* **2010**, *38*, 1685–1694.
(21) Matsunaga, N.; Tsuchimori, N.; Matsumoto, T.; Ii, M. TAK-242 (resatorvid), a small-molecule inhibitor of TLR4 signaling, binds selectively to TLR4 and interferes with interactions between TLR4 and its adaptor molecules. *Mol. Pharmacol.* **2011**, *79*, 34–41.
(22) Bevan, D. E.; Martinko, A. J.; Loram, L. C.; Stahl, J. A.; Taylor, F. R.; Joshee, S.; Watkins, L. R.; Yin, H. Selection, preparation, and evaluation of small-molecule inhibitors of Toll-like receptor 4. *ACS Med. Chem. Lett.* **2010**, *1*, 194–198.

- (23) Joce, C.; Stahl, J. A.; Shridhar, M.; Hutchinson, M. R.; Watkins, L. R.; Fedichev, P. O.; Yin, H. Application of a novel in silico high-throughput screen to identify selective inhibitors for protein–protein interactions. *Bioorg. Med. Chem. Lett.* **2010**, *20*, 5411–5413.
- (24) Bevinakatti, H. S.; Banerji, A. A. Lipase catalysis in organic solvents. Application to the synthesis of (R)- and (S)-atenolol. *J. Org. Chem.* **1992**, *57*, 6003–6005.
- (25) Lee, K. C.; Moon, B. S.; Lee, J. H.; Chung, K.-H.; Katzenellenbogen, J. A.; Chi, D. Y. Synthesis and binding affinities of fluoroalkylated raloxifenes. *Bioorg. Med. Chem. Lett.* **2003**, *11*, 3649–3658.
- (26) Wipf, P.; Weiner, W., S. Enantioselective synthesis and photo-racemization studies of (+)-2-cyclopropyl-7,8-dimethoxy-2H-chromene-5-carboxylic acid methyl ester, an advanced intermediate of a dihydrofolate reductase inhibitor. *J. Org. Chem.* **1999**, *64*, 5321–5324.
- (27) Butera, J. A.; Spinelli, W.; Anantharaman, V.; Marcopulos, N.; Parsons, R. W.; Moubarak, I. F.; Cullinan, C.; Baglit, J. F. Synthesis and selective class III antiarrhythmic activity of novel N-heteroaralkyl-substituted 1-(aryloxy)-2-propanolamine and related propylamine derivatives. *J. Med. Chem.* **1991**, *34*, 3212–3228.
- (28) Bevan, D. E. Selection, Preparation, and Evaluation of Inhibitors of Toll-like Receptor 4. M.S. Thesis, University of Colorado at Boulder, Boulder, CO, U.S., 2010.
- (29) Robin, A.; Brown, F.; Bahamontes-Rosa, N.; Wu, B.; Beitz, E.; Kun, J. F. J.; Flitsch, S. L. Microwave-assisted ring opening of epoxides: a general route to the synthesis of 1-aminopropan-2-ols with anti-malaria parasite activities. *J. Med. Chem.* **2007**, *50*, 4243–4249.
- (30) Lober, S.; Ortner, B.; Bettinetti, L.; Hubner, H.; Gmeiner, P. Analogs of the dopamine D4 receptor ligand FAUC 113 with planar- and central-chirality. *Tetrahedron: Asymmetry* **2002**, *13*, 2303–2310.
- (31) Kemper, S.; Hrobarik, P.; Kaupp, M.; Schlorer, N. E. Jacobsen's catalyst for hydrolytic kinetic resolution: structure elucidation of paramagnetic Co(III)-Salen complexes in solution via combined NMR and quantum chemical studies. *J. Am. Chem. Soc.* **2009**, *131*, 4172–4173.
- (32) Schaus, S. E.; Brandes, B., D.; Larrow, J., F.; Tokunaga, M.; Hansen, K., B.; Gould, A., E.; Furrow, M., E.; Jacobsen, E., N. Highly selective hydrolytic kinetic resolution of terminal epoxides catalyzed by chiral (salen)Co(III) complexes. Practical synthesis of enantioenriched terminal epoxides and 1,2-diols. *J. Am. Chem. Soc.* **2002**, *124*, 1307–1315.
- (33) Ready, J. M.; Jacobsen, E., N. Highly active oligomeric (salen)-Co catalysts for asymmetric epoxide ring-opening reactions. *J. Am. Chem. Soc.* **2001**, *123*, 2687–2688.
- (34) Kang, B.; Chang, S. A facile synthetic route to (+)-allosedamine via hydrolytic kinetic resolution and olefin metathesis. *Tetrahedron* **2004**, *60*, 7353–7359.
- (35) Pérez de Vega, M. J.; García-Aranda, M. I.; González-Muñiz, R. A role for ring-closing metathesis in medicinal chemistry: mimicking secondary architectures in bioactive peptides. *Med. Res. Rev.* [Online early access] DOI: 10.1002/med.20199. Published Online: Jan 14, 2010.
- (36) Fu, G., C.; Nguyen, S., T.; Grubbs, R., H. Catalytic ring-closing metathesis of functionalized dienes by a ruthenium carbene complex. *J. Am. Chem. Soc.* **1993**, *115*, 9856–9857.
- (37) Peng, Z. R.; Zhong, W. H.; Liu, J.; Xiao, P. T. Effects of the combination of hyperbaric oxygen and 5-fluorouracil on proliferation and metastasis of human nasopharyngeal carcinoma CNE-2Z cells. *Undersea Hyperbaric Med.* **2010**, *37*, 141–150.
- (38) Di, L. Profiling drug-like properties in discovery research. *Curr. Opin. Chem. Biol.* **2003**, *7*, 402–408.
- (39) The blood–brain barrier (BBB) permeability and lipophilicity assays were performed by Absorption Systems, Exton, PA.
- (40) Mollnes, T. E.; Brekke, O. L.; Fung, M.; Fure, H.; Christiansen, D.; Bergseth, B.; Videm, V.; Lappgård, K. T.; Köhl, J.; Lambris, J. Essential role of the CSa receptor in *E. coli*-induced oxidative burst and phagocytosis revealed by a novel lepirudin-based human whole blood model of inflammation. *Blood* **2002**, *100*, 1869–1877.
- (41) Fletcher, S.; Turkson, J.; Gunning, P. T. Molecular approaches towards the inhibition of the signal transducer and activator of transcription 3 (Stat3) protein. *ChemMedChem* **2008**, *3*, 1159–1168.
- (42) Wilson, A., J. Inhibition of protein–protein interactions using designed molecules. *Chem. Soc. Rev.* **2009**, *38*, 3289–3300.
- (43) Misko, T. P.; Schilling, R. J.; Salvemini, D.; Moore, W. M.; Currie, M. G. A fluorometric assay for the measurement of nitrite in biological samples. *Anal. Biochem.* **1993**, *214*, 11–16.
- (44) Nussler, A. K.; Glanemann, M.; Schirmeier, A.; Liu, L.; Nussler, N. C. Fluorometric measurement of nitrite/nitrate by 2,3-diaminonaphthalene. *Nat. Protoc.* **2006**, *1*, 2223–2226.
- (45) Jester, B. W.; Cox, K. J.; Gaj, A.; Shomin, C. D.; Porter, J. R.; Ghosh, I. A coiled-coil enabled split-luciferase three-hybrid system: applied toward profiling inhibitors of protein kinases. *J. Am. Chem. Soc.* **2010**, *132*, 11727–11735.